



Nano-scaled diffusional or dislocation creep analysis of single-crystal ZnO

P. H. Lin, X. H. Du, Y. H. Chen, H. C. Chen, and J. C. Huang

Citation: *AIP Advances* **6**, 095125 (2016); doi: 10.1063/1.4964357

View online: <http://dx.doi.org/10.1063/1.4964357>

View Table of Contents: <http://scitation.aip.org/content/aip/journal/adva/6/9?ver=pdfcov>

Published by the *AIP Publishing*

Articles you may be interested in

[Strain-related optical properties of ZnO crystals due to nanoindentation on various surface orientations](#)

J. Appl. Phys. **113**, 183511 (2013); 10.1063/1.4804309

[Local piezoelectric effect on single crystal ZnO microbelt transverse I-V characteristics](#)

Appl. Phys. Lett. **98**, 082105 (2011); 10.1063/1.3555456

[Face dependence of mechanical properties of a single ZnO nano/microrod](#)

J. Appl. Phys. **108**, 056101 (2010); 10.1063/1.3462381

[Reduction of threading dislocations in ZnO/\(0001\) sapphire film heterostructure by epitaxial lateral overgrowth of nanorods](#)

J. Appl. Phys. **104**, 023533 (2008); 10.1063/1.2957082

[Doping and defects in the formation of single-crystal ZnO nanodisks](#)

Appl. Phys. Lett. **89**, 252115 (2006); 10.1063/1.2422899

The advertisement features a blue and orange background with a molecular structure graphic. On the left is a thumbnail of an 'Applied Physics Reviews' journal cover. The main text reads 'NEW Special Topic Sections' in large white letters. Below this, it says 'NOW ONLINE' in yellow, followed by 'Lithium Niobate Properties and Applications: Reviews of Emerging Trends' in white. The AIP Applied Physics Reviews logo is in the bottom right corner.

NEW Special Topic Sections

NOW ONLINE
Lithium Niobate Properties and Applications:
Reviews of Emerging Trends

AIP Applied Physics Reviews

Nano-scaled diffusional or dislocation creep analysis of single-crystal ZnO

P. H. Lin,¹ X. H. Du,^{1,2} Y. H. Chen,¹ H. C. Chen,¹ and J. C. Huang^{1,a}

¹Department of Materials and Optoelectronic Science, National Sun Yat-Sen University, Kaohsiung, Taiwan 804, ROC

²School of Materials Sciences and Engineering, Shenyang Aerospace University, Shenyang 110034, PRC

(Received 17 July 2016; accepted 23 September 2016; published online 30 September 2016)

The nanoindentation time-dependent creep experiments with different peak loads are conducted on *c*-plane (0001), *a*-plane (11 $\bar{2}$ 0) and *m*-plane (10 $\bar{1}$ 0) of single-crystal ZnO. Under nano-scaled indentation, the creep behavior is crystalline orientation-dependent. For the creep on (0001), the stress exponent at low loads is ~ 1 and at high loads ~ 4 . The stress exponents under all loads are within 3–7 for the creep on (11 $\bar{2}$ 0) and (10 $\bar{1}$ 0). This means that diffusion mechanism and dislocation mechanism is operative for different planes and loads. The relative difficulty of dislocations activation is an additional factor leading to the occurring of diffusion creep on the *c*-plane of single-crystal ZnO. © 2016 Author(s). All article content, except where otherwise noted, is licensed under a Creative Commons Attribution (CC BY) license (<http://creativecommons.org/licenses/by/4.0/>). [<http://dx.doi.org/10.1063/1.4964357>]

I. INTRODUCTION

Single-crystal ZnO has been regarded currently as one of the most promising semiconducting materials owing to its relatively wide direct energy gap (about 3.37 eV), high thermal resistivity, high exciton binding energy (~ 60 meV) and chemical stability.^{1,2} As being usually fabricated into low-dimensional piezoelectric devices, it is necessary to measure the mechanical properties of single-crystal ZnO by contact-induced deformation through nanoindentation.^{3–13} In this regard, the time-dependent (so called creep) behavior is especially important in order to assess its mechanical reliability during devices being on service under long-term stress conditions. However, only few researches have been performed on the topic of nanoscale creep behavior of single-crystal ZnO with vertically (0001) orientation.^{12,13} It is found that under the uniaxial compressive stress, the nanoscale creep deformation in single-crystal ZnO nanorods is realized via diffusion mechanism.¹² In contrast, the nanoscale creep strain in single-crystal ZnO under nanoindentation is mainly originated from dislocation-dominated mechanism.¹³

It is generally accepted that the diffusion creep rather than the dislocation-dominated creep is the most common creep mechanism in ceramics.^{14–16} Presumably, the enhanced role of diffusion creep in ceramics is originated from intrinsic factors of ceramics: relatively high Peierls stress in ceramics and the existence of the so-called “space-charge layer” near the surface of ceramics.^{15,16} For the single-crystal ceramics, the happening of diffusion creep is more preferential due to the fact that the deformation in a single crystal often occurs via slip on a single slip plane under the uniaxial stress conditions.¹² Nonetheless, the dislocation-dominated mechanism is responsible for the creep strain of single-crystal ZnO due to the activation of easy multiple slips under the indentation tests.¹³ Thus, it is assumed that there exists a competition between the diffusion mechanism and dislocation mechanism in the course of the creep deformation of ceramics. However, it is not known currently that if the diffusion mechanism can be operative during the nano-scaled creep course of single-crystal ZnO under indentation tests.

^aAuthor to whom correspondences should be addressed. Electronic mail: jacobb@mail.nsysu.edu.tw



Given that the ratio of contacted area and volume probed by indenter is a function of indenter radii, the small radii will produce a much bigger ratio of contacted area and probed volume. This would enhance the diffusion creep behavior under the nanoindentation tests. Hence, in this work, the time-dependent creep experiments were conducted on *c*-plane (0001), *a*-plane ($11\bar{2}0$) and *m*-plane ($10\bar{1}0$) of single-crystal ZnO by nanoindentation with nano-scaled Berkovich tip. By estimating creep stress exponents and activation volume, the creep deformation mechanisms of single-crystal ZnO were figured out under the nanoindentation tests.

II. EXPERIMENTAL PROCEDURE

The specimens used in this experiment are 0.5-mm thick single-crystal Zinc Oxide grown along with [0001] crystallographic direction purchased from MTI Company in the United States. Before tests, the sample surfaces were polished to root mean square roughness less than 10 Å. Nanoindentation tests were conducted using a Nanoindenter XP equipped with a diamond Berkovich tip. The Berkovich tip is triangular pyramidal structure diamond tip with angle about 65.3°. The radius of Berkovich tip used in this study is estimated as 150 nm by Herzian contact indentation analysis of the data obtained from indentation on fused quartz. The Berkovich tip is calibrated by a standard silica sample with over 25 data.

Constant load indentation tests were performed at various stresses in *c*-plane (0001), *a*-plane ($11\bar{2}0$) and *m*-plane ($10\bar{1}0$) of single-crystal ZnO specimens. The specimens were loaded to the peak loads (1 mN, 5 mN and 10 mN) at a fixed loading rate of 0.1 mN/s, held at peak loads for 300 s, and fully unloaded.

III. RESULTS AND DISCUSSION

Figures 1(a,b,c) show the typical creep displacement-holding time curves during nanoindentation creep of *c*-plane (0001), *a*-plane ($11\bar{2}0$) and *m*-plane ($10\bar{1}0$) of single-crystal ZnO under different peak loads, respectively. The creep displacement-holding time curves are parabolic in nature, which are similar to the typical high-temperature creep curves of metals and ceramics.^{12,17–19} Comparing the three figures, it is found that except for the low load of 1 mN, the holding process of high loads (5 and 10 mN) on the *a*-plane ($11\bar{2}0$) and *m*-plane ($10\bar{1}0$) produces larger amount of displacements than that of *c*-plane (0001). This orientation dependency of the displacement indicates that the creep behavior of single-crystal ZnO is not an artifact caused by thermal drift which does not depend on the crystalline orientation.

The creep displacement curves are shown in Figure 2 for the *c*-plane (0001), *a*-plane ($11\bar{2}0$) and *m*-plane ($10\bar{1}0$) samples at 1 mN with different loading rates of 0.01, 0.1 and 1 mNs⁻¹. With increasing loading rate, the creep displacement increases from 9 to 21 nm for the *c*-plane (0001), 12 to 29 nm for *a*-plane ($11\bar{2}0$) and 15 to 38 nm for *m*-plane ($10\bar{1}0$). It is apparent that the creep displacement increases with increasing loading rate. In nanoindentation test, a higher loading rate will exhibit a higher strain rate. Therefore, the higher loading rate would create more defects and displacements during deformation.²⁰

In this work, in an attempt to show if the diffusion can become the responsible mechanism for ceramics under indentation tests, the time-dependent creep experiments were conducted on *c*-plane (0001), *a*-plane ($11\bar{2}0$) and *m*-plane ($10\bar{1}0$) of single-crystal ZnO by nanoindentation with nano-scaled Berkovich tip. To figure out the creep mechanisms of single-crystal ZnO under nanoindentation tests, it is necessary to estimate the values of indicator, i.e. the stress exponents, *n*. It is well documented that *n*=1 for diffusion creep such as the Nabarro-Herring creep (by lattice diffusion) or the Coble creep (by grain boundary diffusion), *n*=2 for grain boundary sliding, *n*=3~8 for dislocation creep in metals.²¹ And these rules are also available to ceramics.²² Figure 3 presents the relationships between strain rate and stress on *c*-plane (0001), *a*-plane ($11\bar{2}0$) and *m*-plane ($10\bar{1}0$) of single-crystal ZnO from nanoindentation creep tests under different peak loads. In general, the stress exponent *n* on *c*-plane (0001), *a*-plane ($11\bar{2}0$) and *m*-plane ($10\bar{1}0$) (the slope of curves in Figure 3) increases with the peak loads.

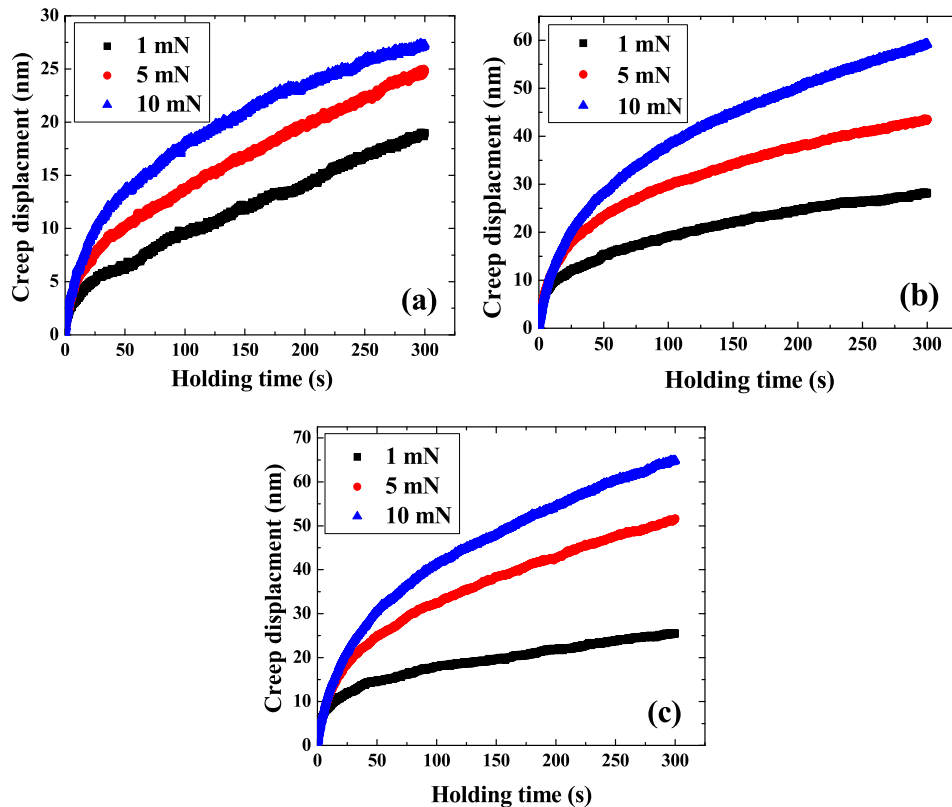


FIG. 1. The creep displacement-holding time curves for the (a) *c*-plane (0001), (b) *a*-plane (11 $\bar{2}$ 0) and (c) *m*-plane (10 $\bar{1}$ 0) single-crystal ZnO under different loads.

The values of n calculated from the stable part of each curves (steady creep) are shown in Figure 4, clearly indicating that the stress exponents all increase with the peak loads for *c*-plane (0001), *a*-plane (11 $\bar{2}$ 0) and *m*-plane (10 $\bar{1}$ 0) of single-crystal ZnO. The stress exponents under the all pre-set peak loads are 3~7 for the *a*-plane (11 $\bar{2}$ 0) and 4~7 for the *m*-plane (10 $\bar{1}$ 0) of single-crystal ZnO, corresponding to the dislocation-dominant creep mechanism. On the other hand, the stress exponents for the *c*-plane (0001) are ~1, ~3 and ~6 at low, medium and high peak loads, respectively, a quite different phenomenon. The distinctive stress exponents for the *c*-plane (0001) of single-crystal ZnO suggest that the diffusion creep and the dislocation-dominant creep mechanisms are operative at low loads and high loads, respectively. This means that under the nanoindentation tests, the diffusion behavior is indeed occurring during the creep course of single-crystal ZnO.

The crystalline orientation-dependent creep behavior can be understood if the activated dislocations in the course of creep deformation on the *c*-plane (0001), *a*-plane (11 $\bar{2}$ 0) and *m*-plane (10 $\bar{1}$ 0) is taken into account. It is known that the relative orientation of the loading direction with respect to the surface determines the shear stresses along the easy-glide planes and in the preferred slip directions. For the *m*-plane configuration, displacement into the crystal is facilitated by slip along the basal plane along the *a*-direction that make $\pm 30^\circ$ angles with respect to the applied load. On the other hand, for indentations on the *c*-plane (0001) of single-crystal ZnO, the applied load is normal to the *a*-direction. Thus, the *c*-plane oriented crystal should have the highest resolved shear stress for the dislocation of the easy-glide basal plane, thus slip along the non-basal planes (pyramidal and prismatic) planes is expected to be activated in addition of the slip along the easy-glide basal planes, as previously reported.^{21,22} The critical resolved shear stress of non-basal planes (*a* and *m*-plane) of ZnO are much higher than that of the easy-glide basal plane, thus, the dislocation nucleating becomes relatively difficult. Thus, it is easier for the dislocation nucleation for the *a*-plane (11 $\bar{2}$ 0) and *m*-plane (10 $\bar{1}$ 0) than *c*-plane (0001) of single-crystal ZnO. As a result, the interfacial diffusion between the nanoindenter tip and the test sample would be more prone to happen

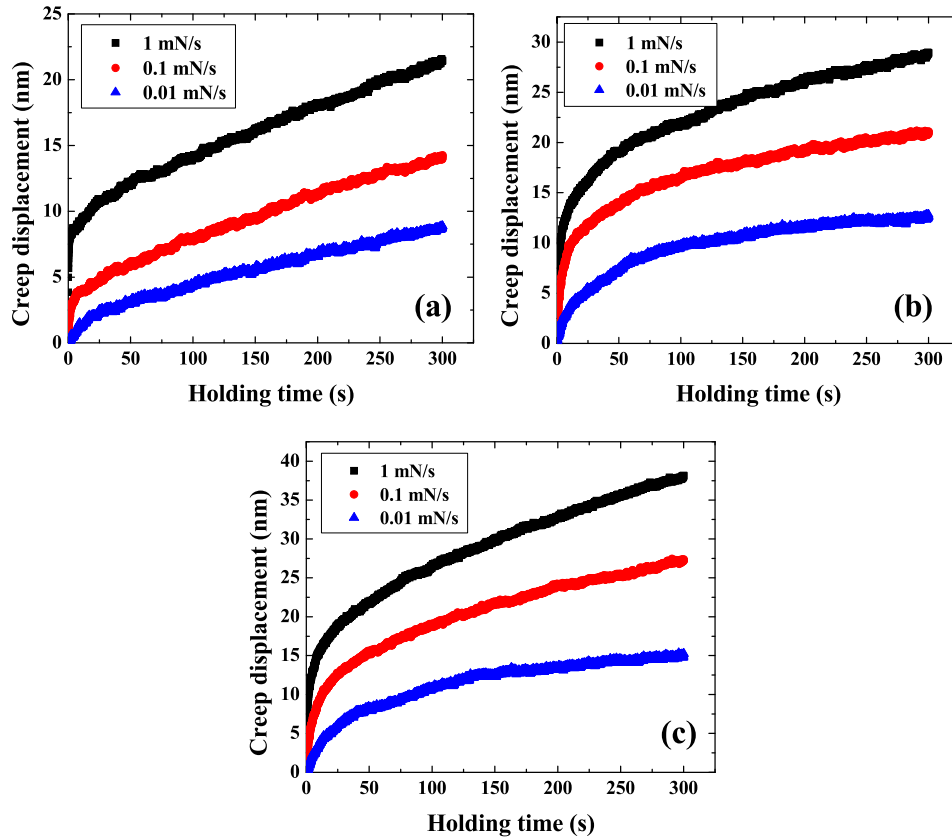


FIG. 2. The creep displacement-holding time curves for the (a) c -plane (0001), (b) a -plane ($11\bar{2}0$) and (c) m -plane ($10\bar{1}0$) single-crystal ZnO under different loading rates.

for the creep on the a -plane ($11\bar{2}0$) and c -plane (0001) than m -plane ($10\bar{1}0$) during nanoindentation process.

The diffusion creep mechanism can be quantitatively interpreted by estimating the strain rate sensitivity m and the activation volume V^* of the creep events:

$$V^* = \sqrt{3}kT \left(\frac{\partial \ln \dot{\epsilon}}{\partial \sigma} \right) = \frac{\sqrt{3}kT}{m\sigma}, \quad (1)$$

where k is Boltzmann's constant and T is the temperature. While the V^* in metals is generally expressed as a fraction of the Burgers vector, it may be possible to describe V^* in ceramics with ionic bonding as a fraction of the ionic volume.⁶ The volume of Zn (V_{Zn}) and O (V_O) ions can be calculated by using the radius of Zn^{+2} ion (0.074 nm) and O^{-2} ion (0.1740 nm). Due to much smaller ion volume, the controlling diffusion species should be the Zn^{+2} ions. The related data on the Zn^{+2} ionic volume, acting dislocation affected volume ($\sim b^3$ for the Burgers vector of $[2\bar{1}\bar{1}0]$), and the activation volume are compiled in Table I.

Note that the V^* of the creep deformation on the c -plane (0001) of single-crystal ZnO under the low peak load can be expressed as $\sim 1V_{Zn}$, which is indicative of the creep deformation occurring *via* motion of individual Zn ions. With increasing load, n starts to increase and V^* also increases, gradually deviating from $1V_{Zn}$ and approaching b^3 . For the medium load level of 5 mN, judging from the n and V^* values, the creep seems to be within the transition region from the diffusion to dislocation controlled mechanism.

In comparison, for the a -plane and m -plane samples, it is found that, independent of load levels, n is consistently 3-7 and V^* being much higher than $1V_{Zn}$ and all approaching b^3 , corresponding to the dislocation-dominant mechanism. Note that the activation volume V^* of c -plane is obviously

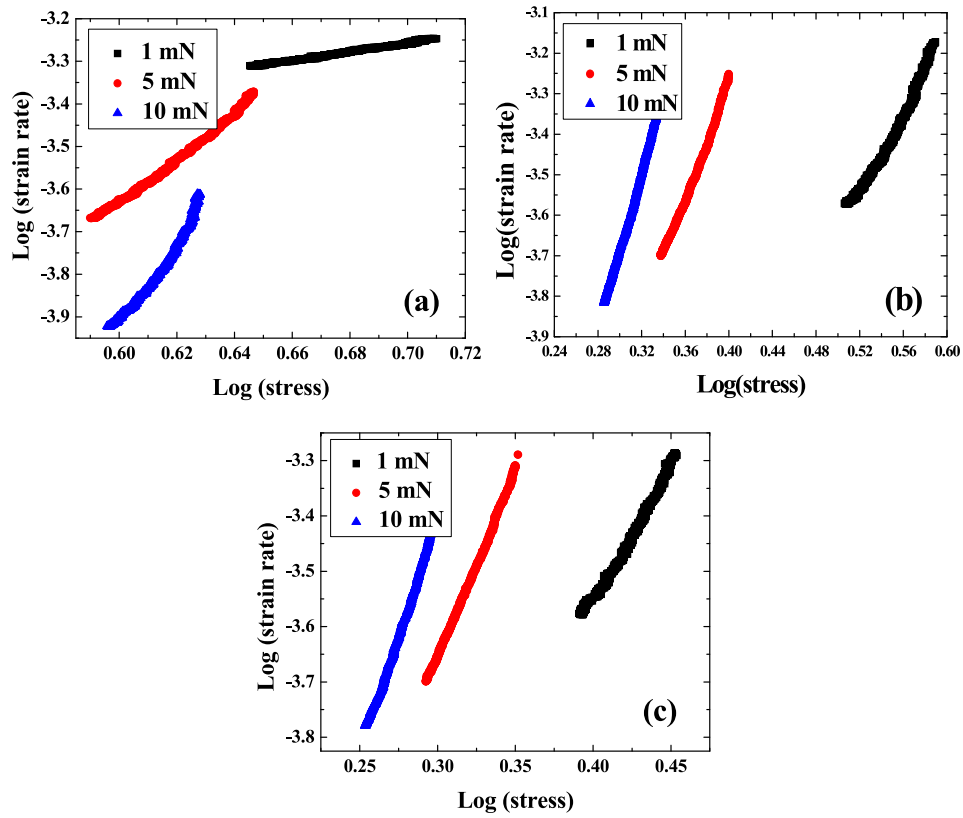


FIG. 3. Typical strain rate-stress curves for the (a) *c*-plane (0001), (b) *a*-plane (11 $\bar{2}$ 0) and (c) *m*-plane (10 $\bar{1}$ 0) single-crystal ZnO under nanoindentation creep.

less than that of *a*-plane and *m*-plane, implying the less activated dislocation motion on the *c*-plane sample.

Another fact should be noted in this study. Compared with the researches of Kim *et al.*,¹³ this work has clearly shown that the more pronounced diffusion creep is observed in smaller indenters. It is known that the diffusive flow of Zn ion is along the interface between the indenter and surface of ZnO single crystal, while the dislocation flow is realized by the dislocation-nucleating heterogeneously in the activated volume under the indenter.^{12,23} The nano-scaled indenter in this study provides much larger ratio of the area of tip-sample contacted interface and the activated volume under the indenter

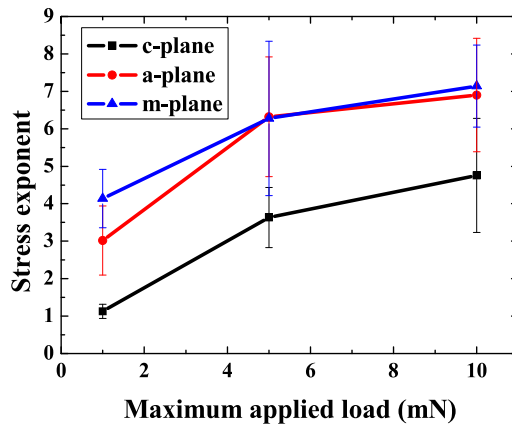


FIG. 4. The variation of the stress exponent as a function of load level for the *c*-plane (0001), *a*-plane (11 $\bar{2}$ 0) and *m*-plane (10 $\bar{1}$ 0) single-crystal ZnO under nanoindentation creep.

TABLE I. Summary of the data on the activation volume Note that the controlling diffusion ion species are Zn^{+2} ions, with the ionic radius of 0.074 nm. The Burgers' vector b for the acting dislocations measures 0.3252 nm (the same as the lattice constant a for ZnO).

Plane	Load (mN)	n	$m (=1/n)$	σ (GPa)	V^* (nm ³)	V_{Zn-ion} (nm ³)	b^3 (nm ³)
<i>c</i> -plane	1	1.0±0.1	1.0±0.06	4.6±0.1	0.0016±0.0003	0.0017	–
	5	3.1±0.2	0.32±0.02	3.8±0.1	0.0060±0.0014	–	0.0344
	10	5.8±0.4	0.17±0.01	3.6±0.1	0.0116±0.0006	–	0.0344
<i>a</i> -plane	1	3.0±0.9	0.27±0.02	3.1±0.1	0.0068±0.0016	–	0.0344
	5	6.3±1.6	0.16±0.06	2.1±0.1	0.0208±0.0044	–	0.0344
	10	6.9±1.5	0.14±0.03	1.9±0.1	0.0260±0.0056	–	0.0344
<i>m</i> -plane	1	4.1±0.8	0.24±0.02	2.5±0.1	0.0143±0.0008	–	0.0344
	5	6.3±2.0	0.16±0.02	2.0±0.1	0.0189±0.0009	–	0.0344
	10	7.1±1.1	0.14±0.02	1.7±0.1	0.0279±0.0009	–	0.0344

than that of micro-scaled indenter as shown in the research of Kim *et al.*¹³ The larger ratio of the area of tip-sample contacted interface and the activated volume is surely favorable for the occurring of diffusion process.

IV. CONCLUSIONS

It is reasonable to assume that under nanoindentation tests, the dislocations creep rather than the diffusion creep is the most common creep mechanism in ceramics. In this work, it is discovered that under nanoindentation tests on the *c*-plane (0001) of single-crystal ZnO with nano-scaled indenter tip, the interfacial diffusion between the nanoindenter tip and the test sample would become the dominant mechanism for the creep strain. It is regarded that the relative difficulty in enabling dislocations motion during the creep on the *c*-plane (0001) is an additional factor leading to the occurring of diffusion process.

ACKNOWLEDGMENTS

The authors gratefully acknowledge the sponsorship from Ministry of Science and Technology of Taiwan, ROC, under the project No. MOST 102-2221-E-110-025-MY3.

- ¹ A. Janotti and C. G. Van de Walle, *Rep. Prog. Phys.* **72**, 126501 (2009).
- ² Ü. Özgür, Y. I. Alivov, C. Liu, A. Teke, M. A. Reshchikov, S. Doğan, V. Avrutin, S. J. Cho, and H. Morkoc, *J. Appl. Phys.* **98**, 041301 (2005).
- ³ G. Feng, W. D. Nix, Y. Yoon, and C. J. Lee, *J. Appl. Phys.* **99**, 074304 (2006).
- ⁴ J. E. Bradby, J. S. Williams, and M. V. Swain, *J. Mater. Res.* **19**, 380 (2004).
- ⁵ R. Juday, E. M. Silva, J. Y. Huang, P. G. Caldas, R. Prioli, and F. A. Ponce, *J. Appl. Phys.* **113**, 183511 (2013).
- ⁶ S. Basu and M. W. Barsoum, *J. Mater. Res.* **22**, 2470 (2007).
- ⁷ R. Juday, E. M. Silva, J. Y. Huang, P. G. Caldas, R. Prioli, and F. A. Ponce, *J. Appl. Phys.* **113**, 1835 (2013).
- ⁸ D. A. Lucca, M. J. Klopstein, R. Ghisleni, and G. Cantwell, *CIRP Ann. Manuf. Technol.* **51**, 483 (2002).
- ⁹ X. Yan, M. Dickinson, J. P. Schirer, C. Zou, and W. Gao, *J. Appl. Phys.* **108**, 056101 (2010).
- ¹⁰ R. Navamathavan, K. K. Kim, D. K. Hwang, S. J. Park, T. G. Lee, G. S. Kim, and J. H. Hahn, *Mater. Lett.* **61**, 2443 (2007).
- ¹¹ T. H. Sung, J. C. Huang, and H. C. Chen, *Appl. Phys. Lett.* **102**, 241901 (2013).
- ¹² Y. J. Kim, W. W. Lee, I. C. Choi, B. G. Yoo, S. M. Han, H. G. Park, W. I. Park, and J. I. Jang, *Acta Mater.* **61**, 7180 (2013).
- ¹³ Y. J. Kim, I. C. Choi, J. A. Lee, M. Y. Seok, and J. I. Jang, *Philosophical Magazine* **95**, 1896 (2015).
- ¹⁴ W. R. Cannon and T. G. Langdon, *J. Mater. Sci.* **23**, 1 (1988).
- ¹⁵ R. M. Cannon and R. L. Coble, *Deformation of ceramic materials* (Plenum Press, New York, 1975).
- ¹⁶ A. H. Chokshi, *J. Eur. Ceram. Soc.* **22**, 2469 (2002).
- ¹⁷ G. E. Dieter, *Mechanical Metallurgy* (McGraw-Hill, London, 1988).
- ¹⁸ F. Wang and K. Xu, *Mater. Lett.* **58**, 2345 (2004).
- ¹⁹ Z. S. Ma, S. G. Long, Y. C. Zhou, and Y. Pan, *Scripta Mater.* **59**, 195 (2008).
- ²⁰ B. G. Yoo, J. H. Oh, Y. J. Kim, K. W. Park, J. C. Lee, and J. I. Jang, *Intermetallics* **18**, 1898 (2010).
- ²¹ J. E. Bradby, S. O. Kucheyev, J. S. Williams, C. Jagadish, M. V. Swain, P. Munroe, and M. R. Phillips, *Appl. Phys. Lett.* **80**, 4537 (2002).
- ²² Y. I. Golovin, A. L. Tyurin, and B. Y. Farber, *J. Mater. Sci.* **37**, 895 (2002).
- ²³ F. Wang, P. Huang, and T. J. Lu, *J. Mater. Res.* **24**, 3277 (2009).